Available online at www.sciencedirect.com
SCIENCE DIRECT®
International Journal of Thermal Sciences 43 (2004) 877–887
International Journal of Thermal Sciences
www.elsevier.com/locate/ijts

Numerical modeling of slot-jet impingement cooling of a constant heat flux surface confined by a parallel wall

Dipankar Sahoo, M.A.R. Sharif *

Aerospace Engineering and Mechanics Department, The University of Alabama, Tuscaloosa, AL 35487-0280, USA

Received 25 May 2003; received in revised form 17 December 2003; accepted 13 January 2004

Available online 27 March 2004

Abstract

The flow and heat transfer characteristics in the jet impingement cooling of a constant heat flux surface have been investigated numerically. Computations are done for vertically downward directed two-dimensional confined slot jets impinging on a constant heat flux surface at the bottom. The principal objective of this study is to investigate the associated heat transfer process in the mixed convection regime. The computed flow patterns and isotherms for various domain aspect ratios and for a range of jet exit Reynolds numbers (100–500) and Richardson numbers (0–10) are analysed to understand the mixed convection heat transfer phenomena. The local and average Nusselt numbers and skin friction coefficients at the hot surface for various conditions are presented. It is observed that for a given domain aspect ratio and Richardson number, the average Nusselt number at the heat flux surface increases with increasing jet exit Reynolds number. On the other hand, for a given aspect ratio and Reynolds number the average Nusselt number does not change significantly with Richardson number indicating that the buoyancy effects are not very significant on the overall heat transfer process for the range of jet Reynolds number considered in this study.

Keywords: Numerical heat transfer; Confined slot jet; Jet impingement cooling; Constant heat flux; Mixed convection

1. Introduction

Impingement cooling is an effective way to generate a high cooling rate in many engineering applications. Impinging jets are often used in heating, cooling, and drying of surfaces. They are employed in paper and textile industries, for cooling of electronic components and turbine blades, drying of veneer, thermal treatment of materials, etc. In steel or gas industries impinging jets are used to cool down the products after rolling. In some circumstances drying rate may be increased by an order of magnitude compared to contact drying. In laser or plasma cutting processes, the application of jet impingement cooling can reduce thermal deformation of products. The impinging jet cooling is an efficient approach for the removal of high power densities encountered in microelectronic devices. In case of a multichip module, uniform cooling, ease of fluid introduction, and removal of fluid from the module in smallest volume are important, which can be achieved by impingement jet cooling.

The heat transfer process in impinging jet cooling may fall in the forced or mixed convection regimes depending on the relative strengths of the inertia/viscous forces and the buoyancy forces involved. The parameter that defines the convection regime is the Richardson number, *Ri*, which is the ratio of the Grashof number and the Reynolds number squared. If the forced convection process is dominant then $Ri \ll 1$ whereas for dominant natural convection, $Ri \gg 1$. If *Ri* is of the order of 1, then both forced and natural convection are comparable and the resulting heat transfer process falls into the mixed convection regime. In many applications of the impinging jet cooling the buoyancy effects may be significant and mixed convection process must be considered for the flow and heat transfer analysis. The interaction between the shear driven and buoyancy driven flow makes the resulting heat transfer process very complex.

Most of the published studies on jet impingement cooling considered forced convection cases [1–3] without taking into account of the buoyancy effects. There is very few reported works in the literature considering mixed convection effects in confined slot jets for impingement cooling. Satyanarayana and Jaluria [4] found that when a heated fluid is discharged at a downward inclination in a laminar slot jet,

* Corresponding author.
E-mail address: msharif@coe.eng.ua.edu (M.A.R. Sharif).

1290-0729/$ – see front matter
doi:10.1016/j.ijthermalsci.2004.01.004

Nomenclature

D_h	hydraulic diameter	Re	Reynolds number
Gr	Grashof number	Ri	Richardson number
k	thermal conductivity	q''	heat flux per unit area
L_x	non-dimensional length of the impinging plate in the x-direction	T	temperature
		U	non-dimensional velocity component in the x-direction
L_y	non-dimensional distance between nozzle exit and impingement plate	V	non-dimensional velocity component in the y-direction
e	non-dimensional length of the heat flux portion	X	non-dimensional coordinate
Nu	Nusselt number	Y	non-dimensional coordinate
P	non-dimensional local pressure	θ	non-dimensional temperature
Pr	Prandtl number		

the jet would eventually have a flow reversal if the exit buoyancy were sufficiently large. The downward penetration of the jet is found to increase with increasing flow inclination, with decreasing jet exit buoyancy and with increasing flow rate. Chen et al. [5] found that the buoyancy introduces a longitudinal pressure gradient, which modifies the flow. Mori [6] analytically predicted the effects of buoyancy for laminar flow over a horizontal surface. In each case of induced decelerating flow there is an upper limit of the mixed convection parameter beyond which the flow will reverse. His results show that the local wall friction coefficient increases sharply in response to a favourable pressure gradient. For the adverse induced pressure gradient, due to negative buoyancy, the skin friction drops sharply. It is to be expected that the strength of adverse longitudinal pressure gradient will ultimately prompt flow separation. In the study of the buoyancy effects on forced laminar convection flow, the effects on transition and the nature of secondary flows were indicated to be closely linked. None of the above-mentioned studies [4–6] address the effects of buoyancy on the local wall friction and heat transfer of an impinging jet. Yuan et al. [7] showed the relative importance of buoyancy on the local wall friction and heat transfer for an impinging jet. Their results also showed the relative importance of buoyancy on the flow structure, the streamwise variation of the flow energy and the surface transport characteristics for the case of two-dimensional laminar impinging jets. Chou and Hung [8] performed numerical calculations to explore the effects of jet Reynolds number, ratio of separation distance to jet width, and jet exit velocity profile on stagnation line boundary layer thickness and local heat transfer characteristics on the isothermal heated surface in confined slot-jet impingement problems without including the buoyancy effects. They proposed new Nusselt number correlations for predicting stagnation line boundary layer thickness and local heat transfer characteristics.

Most of the above mentioned studies considered the hot surface to be cooled as isothermal. In many applications the hot surface may be emitting constant heat flux instead of being isothermal, for example, embedded electronic component on a circuit board. Wadsworth and Mudawar [1] and Wolf et al. [2] reported that the high power electronic chips may dissipate as high as 1–4 $\mathrm{MW\cdot m^{-2}}$ of heat energy. The resulting flow and thermal fields as well as local and overall heat transfer coefficient (Nusselt number) will be different, if not significantly, than the isothermal hot surface condition.

A systematic comprehensive study for mixed convective jet impingement cooling by confined slot jets for a wide range of jet exit Reynolds number and domain aspect ratios have not been done yet, specially for the case when the hot surface has constant heat flux condition. Whenever there is a large temperature difference between the working fluid and the impingement surface containing the constant heat flux source and the flow velocity is not significantly high, there might be some effect of thermal buoyancy force. Since many impingement jet-cooling processes may operate in the mixed convection regime, it is important to understand the effects of buoyancy in the resulting heat transfer and flow physics for designing the cooling system. This is the main motivation and objective of this study.

The rectangular slot in this study is assumed to be large in the spanwise direction. Hence the flow configuration can be considered as a two-dimensional planar jet. Slot jets provide a larger impingement zone and lead to a uniform coolant rejection after impingement. A schematic diagram for the problem configuration is shown in Fig. 1. Due to symmetry of configuration about the vertical y-axis, only the right half of the domain is considered. A downward directed slot jet of width W is placed symmetrically at the middle of the top surface of the domain. The rest of the top surface is adiabatic. All dimensions of the flow domain are normalized by the hydraulic diameter D_h, which is equal to $2W$ for a two-dimensional slot with infinite expanse in the spanwise direction. The bottom wall is maintained at a constant heat flux condition from the symmetry line up to a distance e. The rest of the bottom wall is adiabatic. The length of the domain is L_x while the height is L_y, which signifies the separation distance between the jet exit and impingement plate.

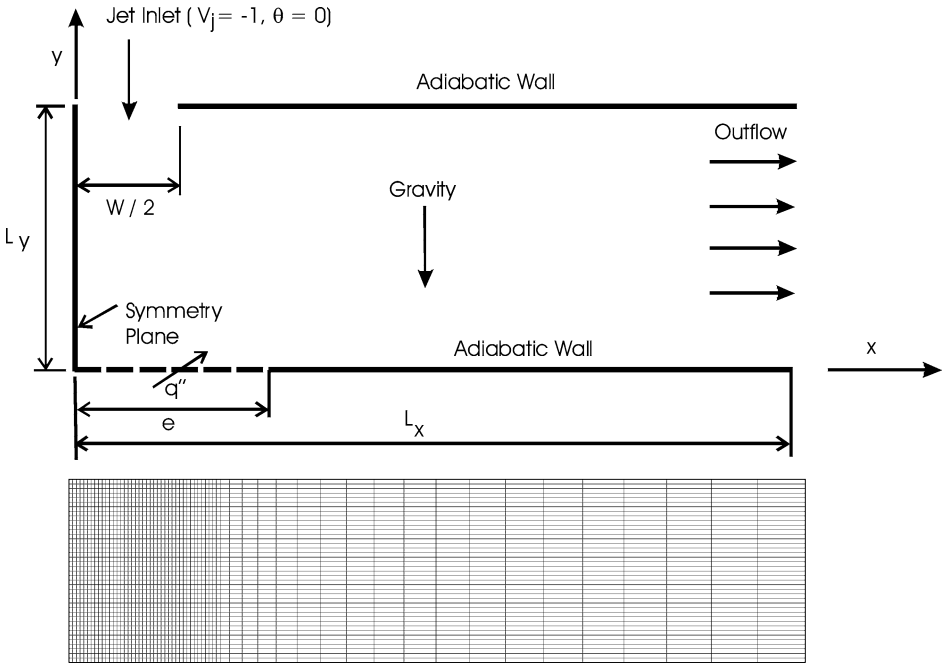

Fig. 1. Schematic diagram of the problem configuration and a representative grid for aspect ratio 4.

2. Mathematical formulation

The non-dimensional mass, momentum, and energy conservation equations for steady, two-dimensional, laminar, incompressible flow with constant fluid properties, after invoking the Boussinesq approximation and neglecting viscous dissipation and radiation effects, are written as

$$\frac{\partial U}{\partial X}+\frac{\partial V}{\partial Y}=0 \tag{1}$$

$$U\frac{\partial U}{\partial X}+V\frac{\partial U}{\partial Y}=-\frac{\partial P}{\partial X}+\frac{1}{Re}\left(\frac{\partial^2 U}{\partial X^2}+\frac{\partial^2 U}{\partial Y^2}\right) \tag{2}$$

$$U\frac{\partial V}{\partial X}+V\frac{\partial V}{\partial Y}=-\frac{\partial P}{\partial Y}+\frac{1}{Re}\left(\frac{\partial^2 V}{\partial X^2}+\frac{\partial^2 V}{\partial Y^2}\right)+\frac{Gr}{Re^2}\theta \tag{3}$$

$$U\frac{\partial \theta}{\partial X}+V\frac{\partial \theta}{\partial Y}=\frac{1}{Pr\,Re}\left(\frac{\partial^2 \theta}{\partial X^2}+\frac{\partial^2 \theta}{\partial Y^2}\right) \tag{4}$$

where U and V are the velocity components in the X and Y directions, respectively, θ is the temperature, and P is the pressure. The scaling parameters are chosen as the average velocity at the jet exit, V_j, the hydraulic diameter of the jet, D_h, a temperature difference defined as $\Delta T = q'' D_h/k$ where q'' is the constant heat flux and k is the thermal conductivity of the fluid, and ρV_j^2 as the characteristic pressure. The jet exit Reynolds number, Re, is defined as $\rho V_j D_h/\mu$, ρ and μ being the fluid density and viscosity, respectively. The Richardson number, Ri, is defined as Gr/Re^2, Gr being the Grashof number which in turn is defined as $g\beta\Delta T D_h^3/\nu^2$ where g is the gravity directed in the negative Y direction, β is the coefficient of thermal expansion, and ν is the kinematic viscosity of the fluid. The Prandtl number, Pr, is defined as ν/α where α is the thermal diffusivity of the fluid.

The boundary conditions at the jet exit are specified as $U=0$, $V=-1$, and $\theta=0$, and for the rest of the adiabatic top wall the conditions are specified as $U=V=0$ and $\partial\theta/\partial Y=0$. At the constant heat flux part of the bottom impingement wall, $0\leqslant X\leqslant e$ (half of the symmetrically placed constant flux heat source), $U=V=0$ and $\partial\theta/\partial y=-1$. This latter condition for dimensionless temperature gradient at the impingement wall is a consequence of defining the characteristic temperature difference $\Delta T = q'' D_h/k$, which also leads to non-dimensional heat flux at the surface to be equal to $1/(Re\,Pr)$. For the rest of the bottom wall, $e\leqslant X\leqslant L_x$, $U=V=0$ and $\partial\theta/\partial y=0$. At the left symmetry wall, $U=0$, $\partial V/\partial X=0$, and $\partial\theta/\partial X=0$. Constant pressure conditions are applied at the right exit boundary where other variables are extrapolated from the inside.

The local Nusselt number at the hot plate is obtained as $Nu(X)=h_X D_h/k=1/\theta(X)|_{\text{hot plate}}$ and the average or overall Nusselt number is obtained by numerical integration as $\overline{Nu}=(\int_0^e Nu(X)\,\mathrm{d}X)/e$, using the trapezoidal rule.

3. Numerical procedure

The set of governing equations are integrated over the control volumes, which produce a set of algebraic equations. The PISO algorithm developed by Issa [9] and Issa et al. [10] is used to solve the coupled system of governing equations. Finite-volume discretization of the governing equations produces a set of algebraic equations, which are solved sequentially by the ADI method. Second-order upwind differencing scheme is used for formulation of the convection contribution to the coefficients in the finite-volume equations. Central differencing is used to discretize the diffusion

terms. The cell center values of the diffusion coefficients are linearly interpolated to get cell face values. The computation is terminated when all of the residuals get below 10^{-5}. The calculations are done using the CFD2000 commercial code where the temperature source term in the momentum equation is incorporated through user subroutines.

4. Results and discussion

For the computations, the jet width, W, is taken as 0.5 so that the hydraulic diameter, D_h, becomes 1. The dimensionless domain length, L_x, is taken as 10 while the height, L_y, is varied. Four different values of L_y; 1, 1.25, 1.67, and 2.5 are considered. This gives the domain aspect ratios, AR, defined as L_x/L_y, of 10, 8, 6, and 4. The working fluid is air with $Pr = 0.71$. The computations are done for 3 different jet exit Reynolds numbers (100, 300, and 500), which is defined in terms of the hydraulic diameter and uniform exit velocity of the jet. The upper limit of 500 for *Re* is based on that suggested by Gauntner et al. [11] and Gardon and Akfirat [12] for laminar flow. They reported that the critical value of *Re* (based on jet width and velocity) for transition to turbulence for impinging slot-jet is about 2000. Other researchers [8,13,14] have used similar range of *Re* for laminar flow analysis of impinging jets. At each Reynolds number, the Richardson number is varied from 0 to 10, thus encompassing a wide range including purely forced convection case ($Ri = 0$) to dominating buoyant convection case. The discrete values of the Richardson number at which

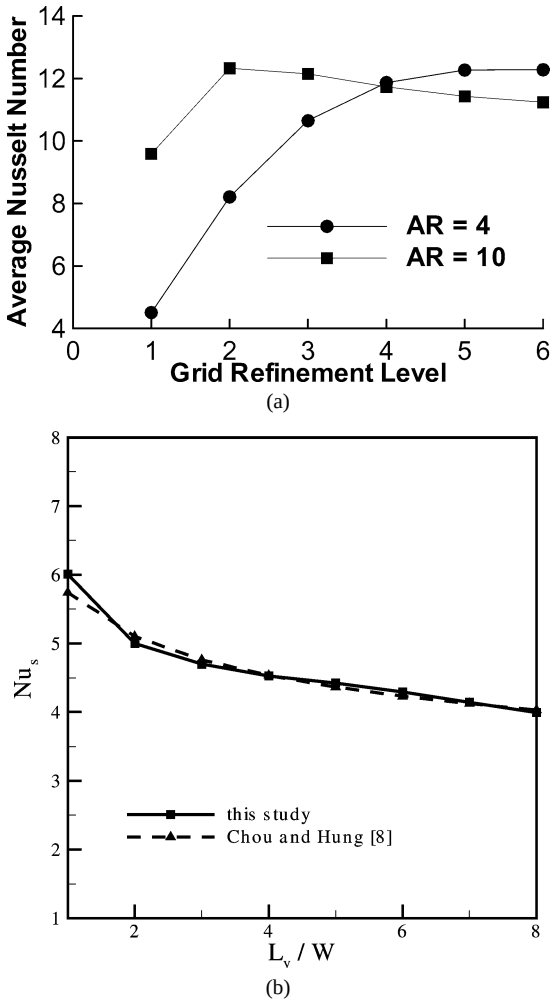

Fig. 2. Convergence of average Nusselt number with grid refinement and comparison of the computed stagnation line Nusselt number, Nu_s, between the present study and those of Chou and Hung [8].

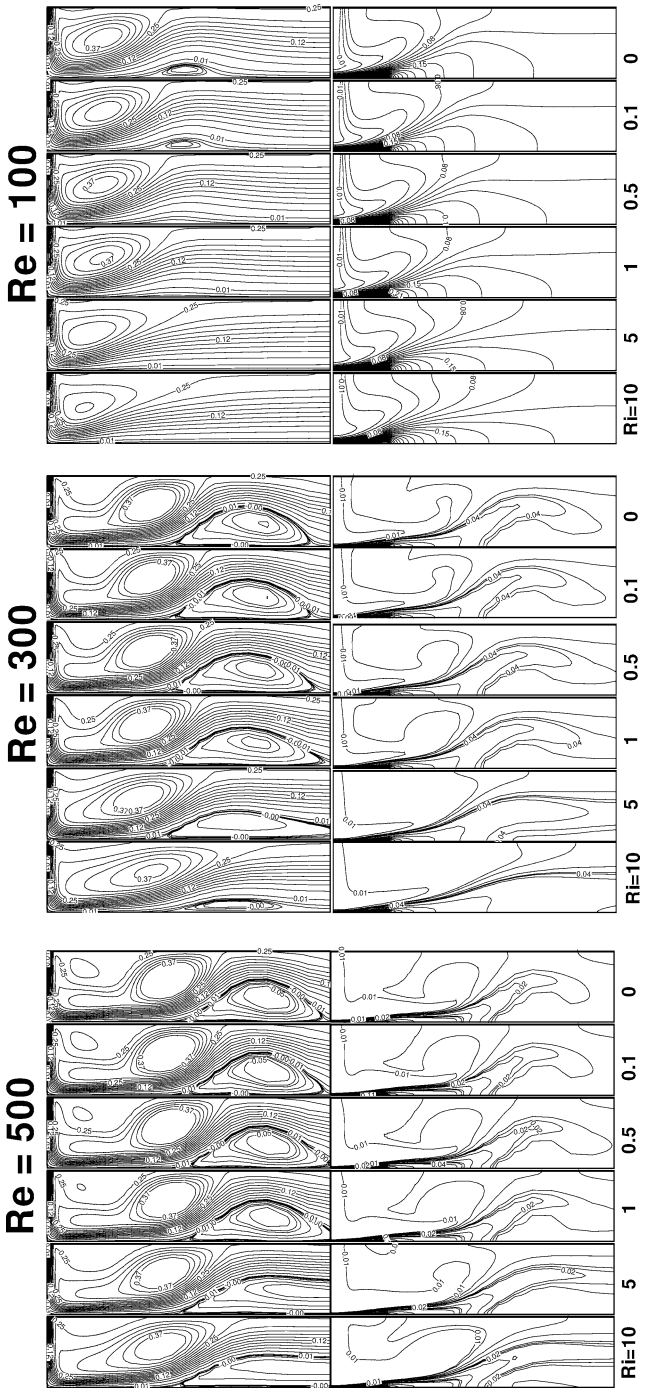

Fig. 3. Streamlines (left) and isotherms (right) for aspect ratio 4.

the computations are done are 0, 0.1, 0.5, 1, 5, and 10. Thus calculations are done for a total 72 different cases.

The mesh is uniformly spaced in the Y direction and also for the heat source part of the bottom surface in the X direction for $0 \leqslant X \leqslant 2$. For $X > 2$, the mesh is stretched in the X direction with an expansion factor of 1.65 towards the domain exit. A representative mesh is also shown in Fig. 1.

A systematic grid refinement study, according to a grid refinement scheme shown in Table 1, is conducted to obtain grid independent solutions. Computations are done for aspect ratio 4 and 10 at $Re = 500$ and $Ri = 1$ while the grid is refined. Fig. 2 as well as Table 1 show the convergence of the average Nusselt number at the heat flux surface with grid refinement from which it is observed that grid level 5 (grid 5) produced almost grid independent solutions. This grid resolution is therefore used for all subsequent computations.

Due to the lack of suitable experimental data on the particular problem along with its associated boundary conditions investigated in this study, validation of the predictions against experiment could not be done. However, the numerical results of the study by Chou and Hung [8], whose geome-

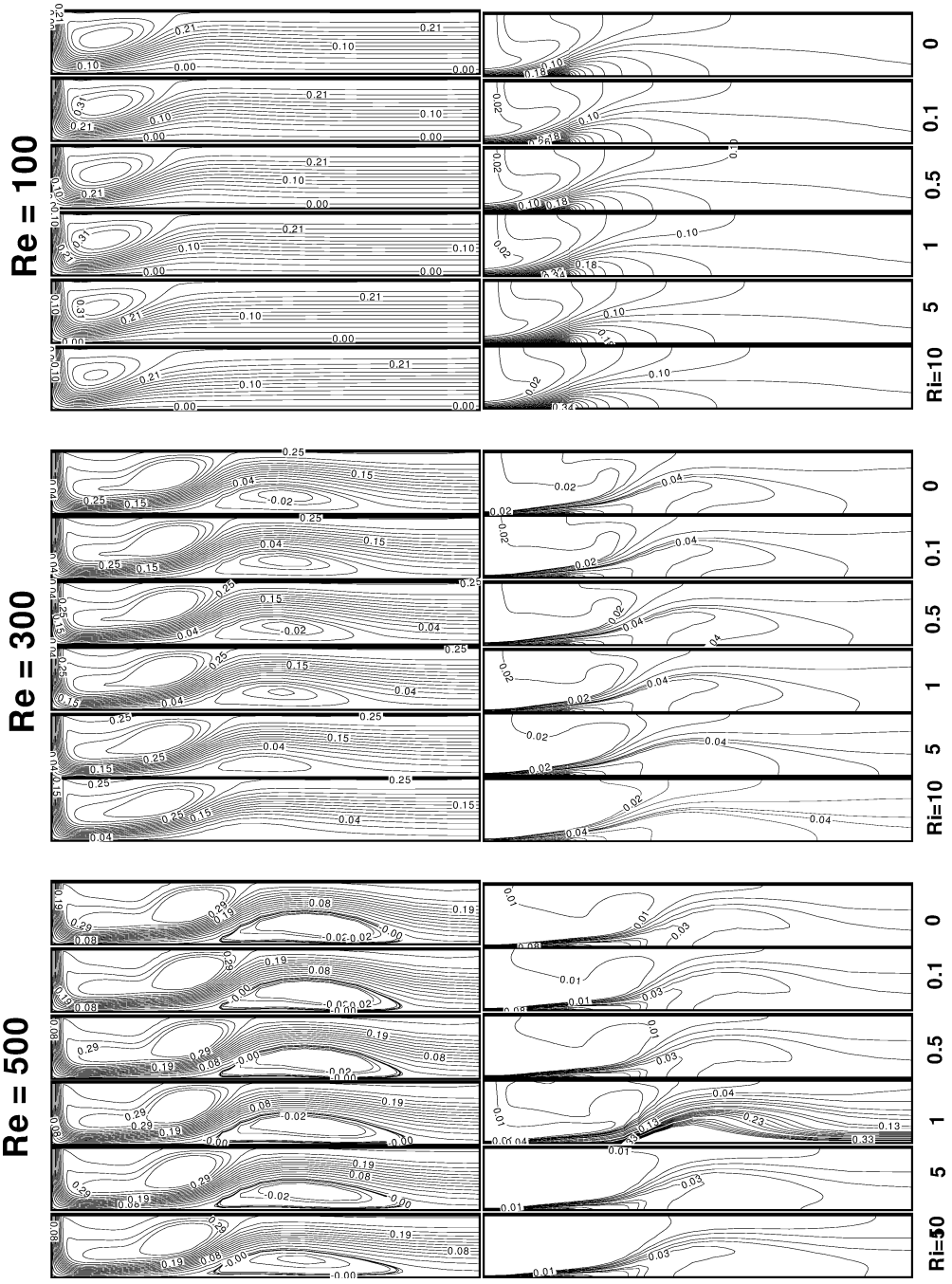

Fig. 4. Streamlines (left) and isotherms (right) for aspect ratio 6.

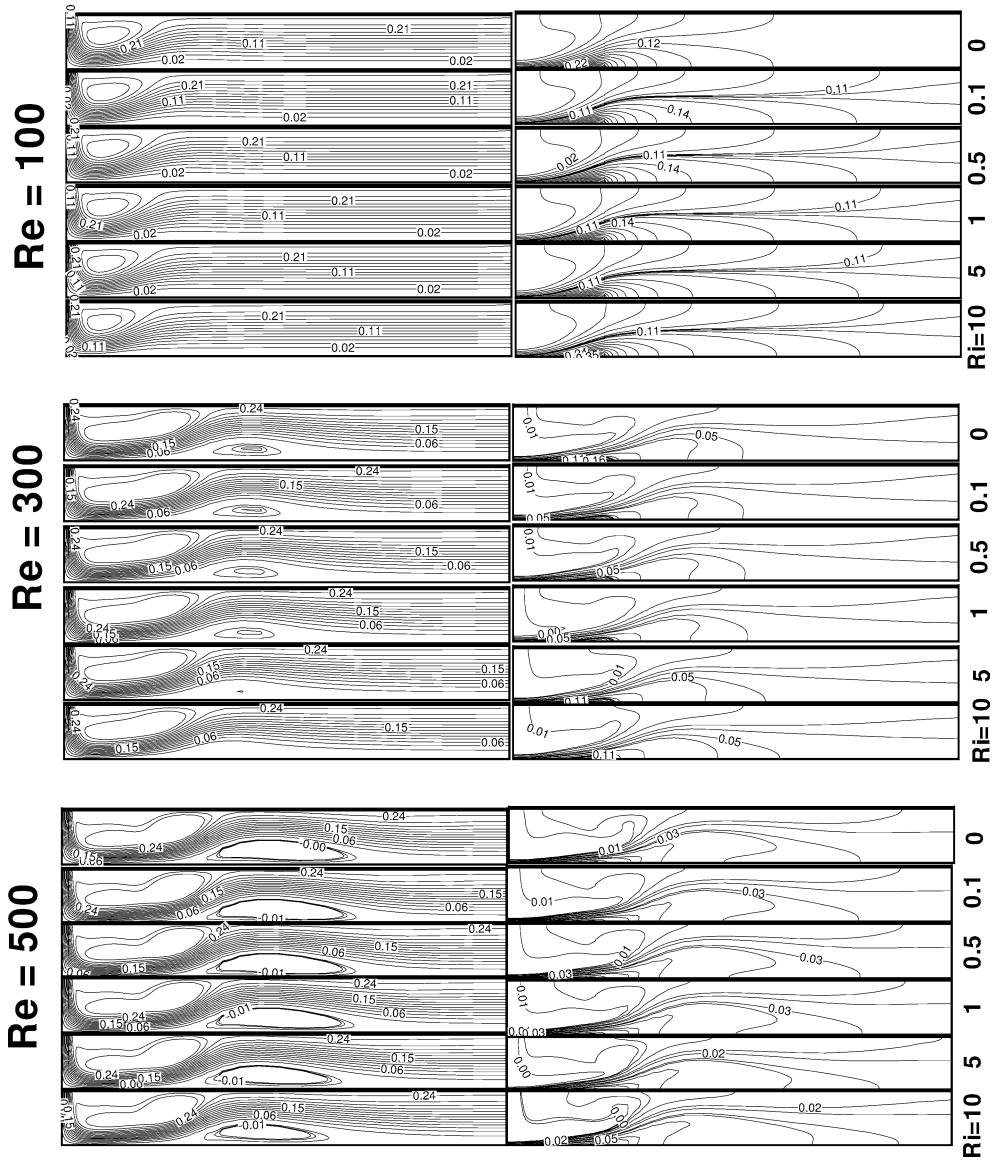

Fig. 5. Streamlines (left) and isotherms (right) for aspect ratio 8.

Table 1
Grid refinement scheme

Grid refinement level	Y direction uniform spacing	X direction		Average Nu	
		$0 \leqslant X \leqslant 2$ uniform spacing	$X > 2$ stretched	$AR = 4$	$AR = 10$
Grid 1	8	8	4	4.51	9.59
Grid 2	16	16	8	8.21	12.33
Grid 3	24	24	12	10.65	12.15
Grid 4	32	32	16	11.87	11.73
Grid 5	40	40	20	12.27	11.43
Grid 6	48	48	24	12.28	11.23

try and flow parameters are quite similar to the present study are reproduced using the present computer code. Chou and Hung [8] used a different computational procedure (stream function-vorticity method with SIMPLEC algorithm). The Nusselt number at stagnation line predicted by the present computer code for zero buoyancy and isothermal hot surface condition is compared with the calculations of Chou and Hung [8] in Fig. 2. The agreement is found to be very good which indicates the validity of the present computation to some extent.

The predicted streamlines and isotherms at different Reynolds and Richardson numbers for domain aspect ra-

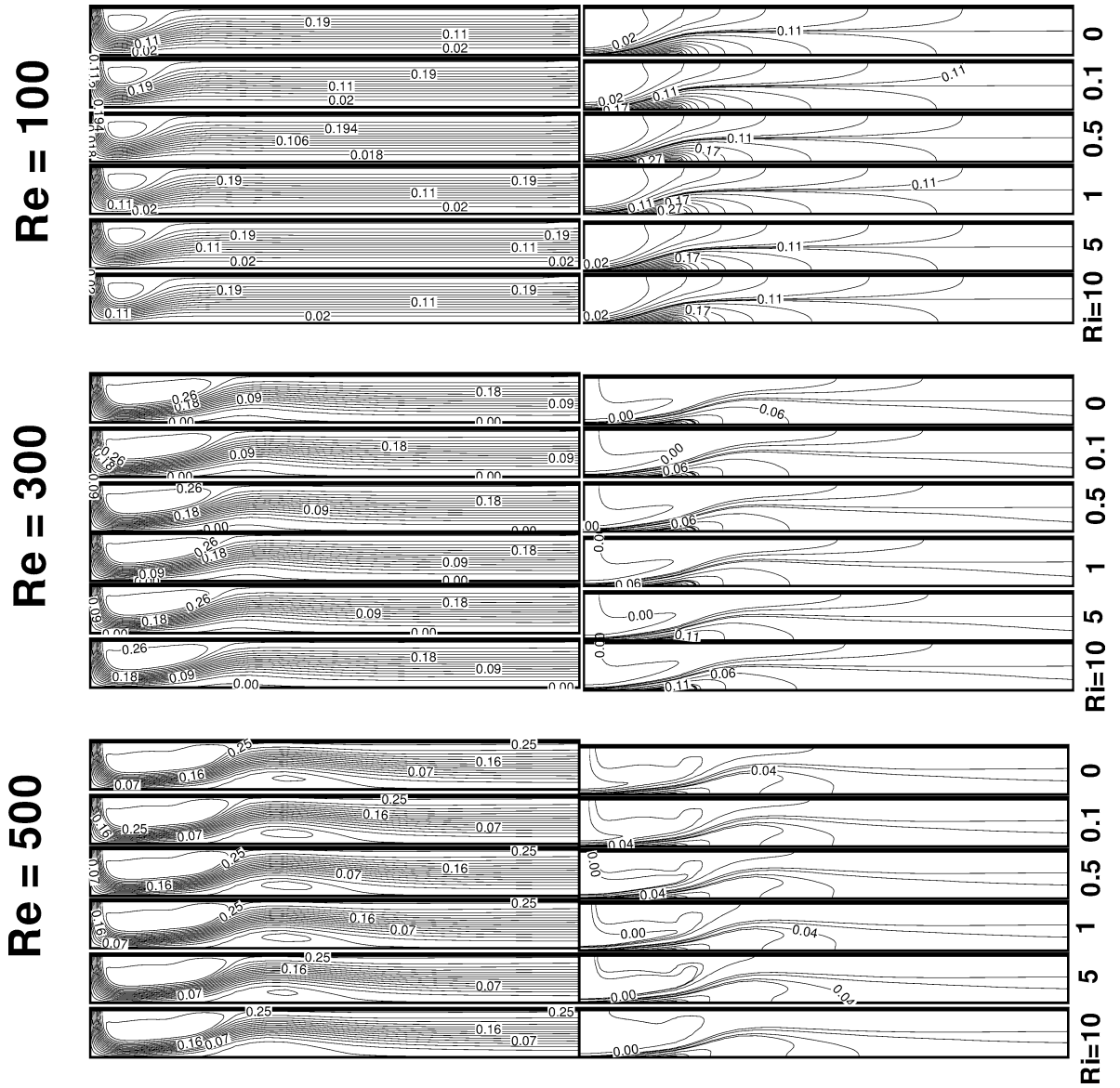

Fig. 6. Streamlines (left) and isotherms (right) for aspect ratio 10.

tios of 4, 6, 8, and 10 are shown in Figs. 3–6, respectively. From these figures it is observed that, at any particular aspect ratio and Reynolds number there is a marked change in flow patterns and isotherms as the flow regime changes from dominant forced convection ($Ri \sim 0$) to increasing buoyancy with increasing Richardson number. As the jet impinges unto the bottom plate a counterclockwise primary vortex is generated near the upper plate adjacent to the jet due to entrainment. As the Reynolds number is increased a clockwise secondary vortex is generated near the impingement plate, which is smaller than the primary one and it is also weaker in terms of rotational intensity. With the increase in Reynolds number the size of the secondary vortex also increases. There is some flow reversal at the domain exit for higher Reynolds number and Richardson number for aspect ratio 4. Since constant pressure condition is imposed on that boundary, this did not produce any numerical problem. The length of the primary vortices decrease as the *AR* is increased for the range of the *Re* and *Ri* considered. For a given *AR* it can be observed that the centers of both the primary and secondary vortices move downstream as *Re* is increased. For all the aspect ratios and range of Richardson numbers considered, flow separation at the bottom surface occurs at larger Reynolds number due to the secondary vortices. For a particular aspect ratio and a Reynolds number the effect of buoyancy is distinctly observed. As the Richardson number increases the strength and length of the secondary vortices reduces as shown in the streamline plots.

For the isotherm plots, it is observed that for a particular *AR* and *Re*, the isotherms become denser towards the heat source portion as the *Ri* (the buoyancy effect) increases. The temperature gradient decreases away from the region of impingement until the last part of the heat flux portion where it is slightly increased. It is also noticed that for a

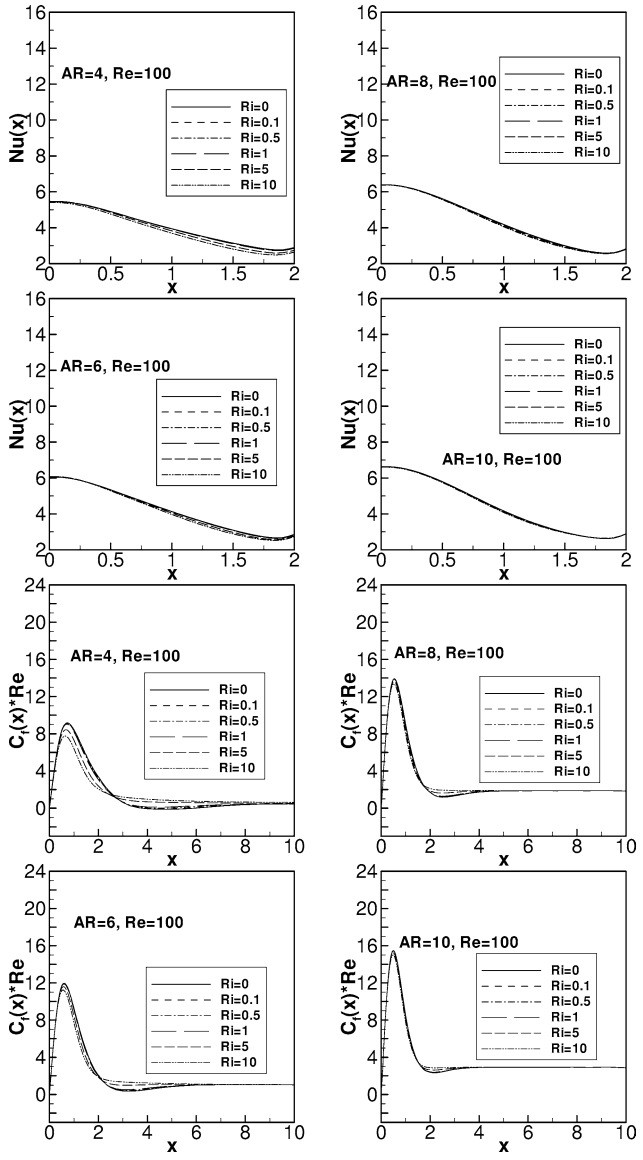

Fig. 7. Variation of the local Nusselt number and skin friction coefficient at the bottom surface for $Re = 100$.

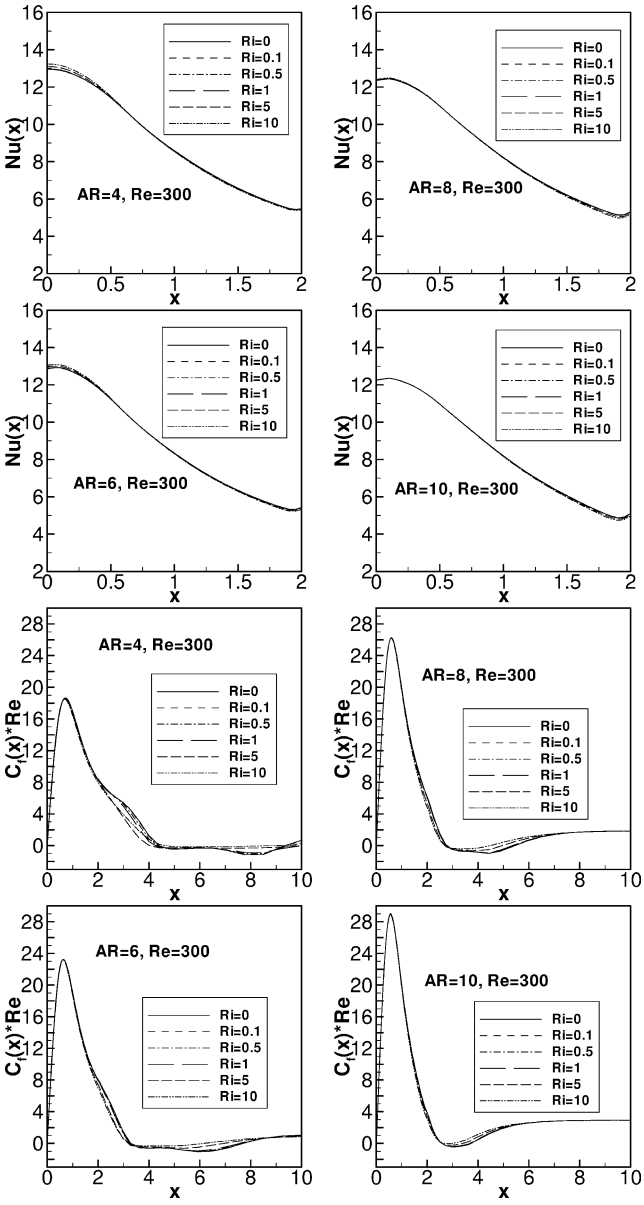

Fig. 8. Variation of local the Nusselt number and skin friction coefficient at the bottom surface for $Re = 300$.

given *AR* and *Re*, the average temperature of the flow domain decreases as *Ri* increases making the domain cooler.

Figs. 7–9 show the variation of local Nusselt number, $Nu(X)$, along the heat flux part of the impingement plate for the whole range of parameters considered in this study. It is observed that for $0 \leqslant X \leqslant 2$ the effect of buoyancy (*Ri*) on the local Nusselt number is insignificant for the range of Reynolds number considered. However, from the figures it is evident that for low Reynolds number ($Re = 100$) and higher Richardson number the Nusselt number decreases very slightly. This effect is diminished as the aspect ratio and Reynolds number are increased. For a particular aspect ratio, at higher Reynolds numbers the local Nusselt number increase slightly to a maximum and then decreases along the surface. Since the local Nusselt number is reciprocal of the dimensionless surface temperature, this indicates that the surface temperature is minimum around $X = 0.1$ (not at the stagnation line), and then increases along the surface.

In a jet impingement flow buoyancy affects both the heat transfer coefficient and skin friction coefficient on the impingement surface. As a part of investigation, it is desired to show the effect of Richardson number on skin friction coefficient C_f. Figs. 7–9 also show the variation of C_f, multiplied by the Reynolds number, along the hot surface for the range of parameters considered. The local skin friction factor increases sharply from zero at the stagnation point to a maximum value in a short distance near the impingement region and then decreases with the streamwise distance, X. For the case of downward facing jet the buoyancy forces work against the flow. For large

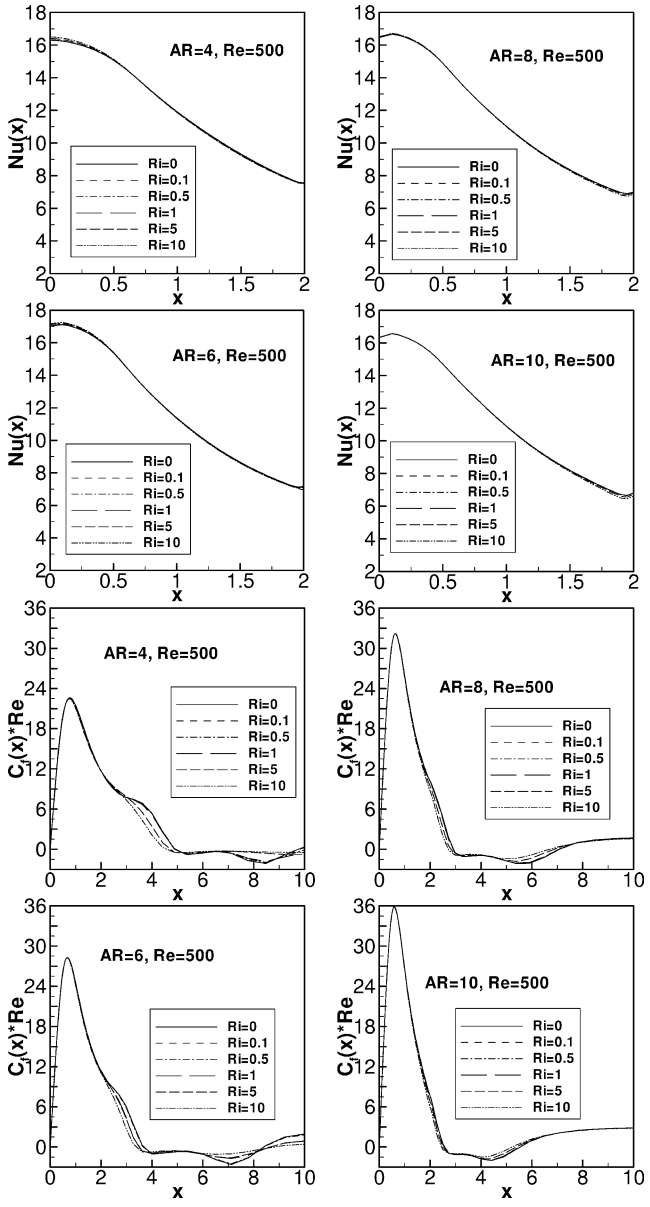

Fig. 9. Variation of the local Nusselt number and skin friction coefficient at the bottom surface for $Re = 500$.

Richardson numbers the impinging velocity is reduced, as is the wall friction. As the value of *Ri* becomes sufficiently small, C_f is slightly reduced. As the secondary vortex is created the flow separation takes place and hence local skin friction increases with increase in Richardson number making the effect of buoyancy noticeable. Towards the outflow the C_f values becomes almost independent of the Richardson number. This trend is observed as the distance between the isothermal plate and jet exit is reduced. Another important point to be noted is negative values of C_f occur indicating the condition of flow recirculation. For a particular aspect ratio the value of skin friction coefficient increases with increase in Reynolds number. For a given *Re*, the peak value of C_f also increases with increase in aspect ratio.

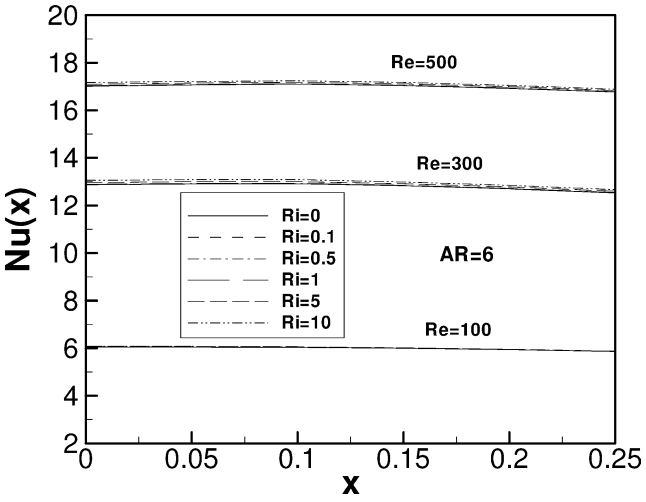

Fig. 10. Close-up view of the variation of local Nusselt number near the impingement region.

A close-up view of the variation of the local Nusselt number along the heat source at the impingement region is shown in Fig. 10 for a representative aspect ratio of 6 for the range of *Re* and *Ri* considered. It is observed that for a particular Reynolds number, the Nusselt number decreases in the region $0.01 < X < 0.2$ starting with a higher value very close to stagnation line. This is because of the high convection process going on at the impingement region. This process gradually becomes weak and the local Nusselt number almost stays the same. However for $Re = 300$ and 500, with an increase in *Ri* there is a slight increase in the Nusselt number at the jet impingement region. This trend is reversed towards the end of the heat source, which is not shown in the above figure. Similar trend is also observed for $AR = 4$, 8 and 10.

Fig. 11 shows the variation of overall or average Nusselt number, $\overline{Nu}$ at the heat source with Richardson number for the different aspect ratios and Reynolds numbers considered. It is observed that the overall Nusselt number increases significantly with Reynolds number. It is however, also observed that $\overline{Nu}$ decreases slightly with increase in Richardson number for any particular set of aspect ratio and Reynolds number considered. This indicates that the effect of buoyancy on the overall heat transfer process is insignificant for any specific set of aspect ratio and jet exit Reynolds number even though the evolution of the flow and thermal field for the whole domain with increasing Richardson number is noticeable. This rather unexpected finding can be attributed to the constant flux boundary condition at the heated surface and the range of relatively higher jet exit Reynolds number (100–500) investigated in this study. The effect of the buoyancy on overall Nusselt number is not significant at these higher Reynolds number. It may be significantly noticeable for low exit jet Reynolds number. In order to verify this statement, simulations are repeated at a jet exit Reynolds number of 30 with aspect ratio 6 and varying Richardson number from 0 to 10 and

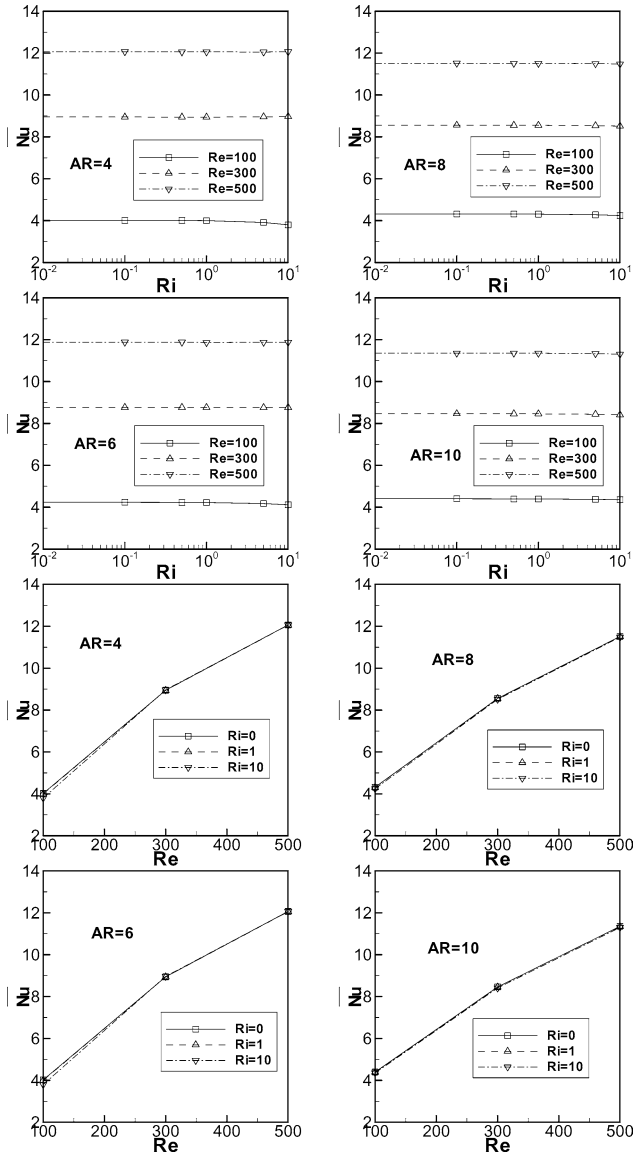

Fig. 11. Variation of average Nusselt number at the hot surface with Richardson number and Reynolds number.

it is found that the overall Nusselt number decreases by 41%, whereas at higher Reynolds number (100–500) the change in overall Nusselt number is found to be less than 3% when the Richardson number is varied from 0 to 10. On the other hand, when simulations are done for a higher jet exit Reynolds number of 300 with a very high Richardson number of 100, the overall Nusselt number changes by only 2%.

It is also of interest to investigate the effect of the separation distance from the jet exit to the impingement plate, L_y, on the heat transfer process. The variation of the overall Nusselt number has been plotted against L_y, in Fig. 12. It is observed that for higher Reynolds number $\overline{Nu}$ increases slightly with L_y. It is also observed that the effect of Richardson number is more noticeable at lower Reynolds number.

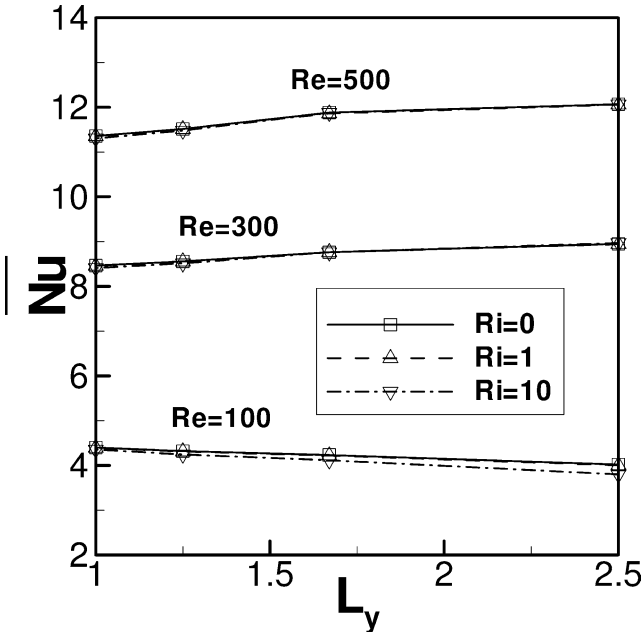

Fig. 12. Variation of overall Nusselt number at the hot surface with L_y.

5. Conclusions

Laminar mixed convective cooling of a constant flux hot surface by confined slot jet impingement is studied in detail through two-dimensional numerical simulation for a wide range of domain aspect ratio, jet exit Reynolds number, and Richardson number. The mixed convection effect, characterized by the Richardson number, increases as the Richardson number is gradually increased from zero (purely forced convection). Predicted flow and thermal fields are presented in the form of streamlines and isotherms. The variation of the local and overall Nusselt number and skin friction coefficient at the hot surface is presented for the range of parameters considered.

There are noticeable changes in the flow and thermal fields as the Richardson number changes for a particular set of jet exit Reynolds number and domain aspect ratio. Flow separation along the impingement surface occurs for small Richardson number depending on the aspect ratio and jet Reynolds number.

The local Nusselt number along the hot plate varies slightly with Richardson number for a particular set of domain aspect ratio and jet Reynolds number. However, the overall Nusselt number at the hot plate does not change significantly with Richardson number for the range of jet exit Reynolds number considered, despite noticeable changes in the flow and thermal field in the whole domain. The insignificant effect of the Richardson number on the overall Nusselt number is attributed to the constant flux boundary condition at the heated surface and the range of jet exit Reynolds numbers (100–500) that are considered moderately high. At low Reynolds number ($Re = 30$), the effect of Richardson number variation is significant.

The skin friction coefficient increases rapidly from zero at the stagnation line to a peak very close to the stagnation line and then drops quickly, which is typical for impinging jet problem. Slight variation of the skin friction coefficient is observed with increasing Richardson number and decreasing aspect ratio.

References

[1] D.C. Wadsworth, I. Mudawar, Cooling of a multichip electronic module by means of confined two-dimensional jets of dielectric liquid, J. Heat Transfer 112 (1990) 891–898.
[2] D.H. Wolf, R. Viskanta, F.P. Incropera, Local convective heat transfer from a heated surface to a planar jet of water with a nonuniform velocity profile, J. Heat Transfer 112 (1990) 899–905.
[3] J.Y. San, C.H. Huang, M.H. Shu, Impingment cooling of a confined circular air jet, Internat. J. Heat Mass Transfer 40 (1997) 1355–1364.
[4] S. Satyanarayana, Y. Jaluria, A study of laminar buoyancy jets discharged at an inclination to the vertical buoyancy force, Internat. J. Heat Mass Transfer 25 (1982) 1569–1577.
[5] T.S. Chen, E.M. Sparrow, A. Mucoglu, Mixed convection in boundary layer flow on a horizontal plate, J. Heat Transfer 99 (1977) 66–71.
[6] Y. Mori, Buoyancy effects in forced laminar convection flow over a horizontal flat plate, J. Heat Transfer 83 (1961) 479–482.
[7] T.D. Yuan, J.A. Liburdy, T. Wang, Buoyancy effects on laminar impinging jets, Internat. J. Heat Mass Transfer 31 (1988) 2137–2145.
[8] Y.J. Chou, Y.H. Hung, Impingement cooling of an isothermally heated surface with a confined slot jet, J. Heat Transfer 116 (1994) 479–482.
[9] R.I. Issa, Solution of the implicitly discretized fluid flow equations by operator-splitting, J. Comput. Phys. 62 (1985) 40–65.
[10] R.I. Issa, B. Ahmadi-Befrui, K.R. Beshay, A.D. Gosman, Solution of the implicitly discretized reacting flow equations by operator-splitting, J. Comput. Phys. 93 (1991) 388–410.
[11] J.W. Gauntner, J.N.B. Livingwood, P. Hrycak, Survey of literature on flow characteristics of a single turbulent jet impinging on a flat plate, NASA TN D-5652, 1970.
[12] R. Gardon, J.C. Akfirat, Heat transfer characteristics of impinging two-dimensional air jets, J. Heat Transfer 88 (1966) 101–108.
[13] H.S. Law, J.H. Masliyah, Numerical prediction of the flow field due to a confined laminar two-dimensional submerged jet, Comput. Fluids 12 (1984) 199–215.
[14] S. Al-Sanea, Anumerical study of the flow and heat transfer characteristics of an impinging laminar slot-jet including crossflow effects, Internat. J. Heat Mass Transfer 35 (1992) 2501–2513.